Inorganica Chimica Acta 487 (2019) 456–464

Contents lists available at ScienceDirect

Inorganica Chimica Acta

journal homepage: www.elsevier.com/locate/ica

Research paper

Ni^{2+}–Fe^{3+} cyanometallate structures covalently embedded in silica: Influence of the blocking ligand at Ni^{2+}

Elisabeth Felbermair[a], Johanna Akbarzadeh[b], Herwig Peterlik[b], Andrey Sidorenko[c], Silke Paschen[c], Ulrich Schubert[a,*]

[a] Institute of Materials Chemistry, Vienna University of Technology, Getreidemarkt 9, 1060 Wien, Austria
[b] Faculty of Physics, University of Vienna, Boltzmanngasse 5, 1090 Wien, Austria
[c] Institute of Solid State Physics, Vienna University of Technology, Wiedner Hauptstraße 8-10, 1040 Wien, Austria

ARTICLE INFO

Keywords:
Sol-gel materials
Cyanometallates
Silica
Small-angle scattering

ABSTRACT

Ni(II)/Fe(III) cyanometallate structures with $Si(OR)_3$-substituted bis(2-aminoethyl)-1,3-propanediamine or 1,4,8,11-tetraazacyclotetradecane (cyclam) blocking ligands at Ni(II) were prepared and embedded in SiO_2 by means of sol-gel processing with $Si(OEt)_4$. The cyanometallates were microcrystalline before sol-gel-processing, and a double-chain structure is proposed for the silyl-substituted $[Ni(tetramine)]_3[Fe(CN)_6]_2$ derivatives. The 3D arrangement is lost during sol-gel processing, although Fe(III)−C≡N−Ni(II) structures are retained in the gels, as proven by FTIR and SWAXS studies. The obtained gels show paramagnetic behavior.

1. Introduction

In cyanometallate 1D, 2D or 3D coordination polymers, transition metals of the same or different kind are bridged by cyano ligands [1–3]. Exchange interaction through M−N≡C−M′ bridges often results in interesting magnetic properties [4,5]. The structures of cyanometallates, and concomitantly the (magnetic) properties, can be modified by varying the metal centers, the auxiliary ligands or the M:M′ ratio, or by introducing counter ions or solvent/guest molecules. Cyanometallates are typically obtained as single crystals or powders, which, however, are difficult to process for utilization of their magnetic properties.

Incorporation of cyanometallate structures in sol-gel materials could offset this disadvantage. The latter are known for their manifold processing possibilities (to obtain ceramic bodies, aerogels, fibers, coatings, particles or powders), mild synthesis conditions and the possibility to prepare hybrid materials, in which compounds with different structural, physical or processing characteristics are synergistically combined. Physical containment of molecular or nanosized objects in a gel matrix is the easiest possibility. In the case of Prussian blue structures, this has been done by stepwise impregnation of pre-formed silica with a metal ion and $[Fe(CN)_6]^{3-}$ whereby the cyanometallate structures are formed within the pores of the silica matrix ([6,7] as more recent references). The dispersion of the guest species, however, is easier controlled and the stability of the hybrid materials is higher if the components from which the hybrid material is built are connected with each other by covalent bonds. To this end, Cu^{2+} ions were coordinated to a triazole unit covalently bonded to pre-formed silica, followed by reaction with $[Fe(CN)_6]^{3-}$ [8].

We are reporting a completely different approach. Instead of creating the cyanometallate structures in or on silica, we start from pre-formed cyanometallates in which the blocking ligand is substituted by $Si(OR)_3$ groups. Such derivatives of the blocking ligands allow incorporation of the cyanometallate structures on the silica network upon sol-gel co-processing with $Si(OR)_4$. In the resulting hybrid materials, the cyanometallate structures are covalently bonded to the silica network. The aim of our work is to study whether and how the $Si(OR)_3$-substituted blocking ligands influence the formation of cyanometallate compounds and the properties of materials obtained thereof.

Ni(II)/Fe(III) cyanometallates were selected for this study not only because of their interesting magnetic properties, such as single molecule magnets, magnetic sponges, photo-switches etc., but also because Ni(II) is usually coordinated by blocking ligands. The latter ensure that only two cyano groups complete the octahedral coordination of Ni(II) and therefore a low-dimensional (1D/2D) network is favored. Some blocking ligands reported in the literature are shown in Fig. 1 and document the strong inclination to di- and tetramines. The cyanometallates are easily obtained by reaction of $[Fe(CN)_6]^{3-}$ with either

* Corresponding author.
E-mail address: ulrich.schubert@tuwien.ac.at (U. Schubert).

https://doi.org/10.1016/j.ica.2018.12.019
Received 16 October 2018; Received in revised form 8 December 2018; Accepted 8 December 2018
Available online 10 December 2018

$[Ni(diamine)_2]^{2+}$ or $[Ni(tetramine)_2]^{2+}$.

In a proof-of-principle study we had used $[Ni(AEAPTS)_2]^{2+}$ (AEAPTS = *N*-(2-aminoethyl)-3-amino-propyltrimethoxysilane, a $Si(OMe)_3$-substituted derivative of ethylene diamine). Sol-gel processing of $[Ni(AEAPTS)_2]_3[Fe(CN)_6]_2$ resulted in incorporation of the cyanometallate in silica. The obtained material was magnetically ordered below 22 K with an effective magnetic moment μ_{eff} of 4.46 μ_B at room temperature, a maximum of 8.60 μ_B at ~15 K and a narrow hysteresis at 2 K, with a saturation remanence of about 300 emu mol^{-1} and a coercitivity of 0.03 T [9].

In the current article we compare the results of this preliminary study with that of Ni(II) complexes coordinated by $Si(OMe)_3$-substituted derivatives of the tetradentate ligands 2,3,2-tetramine and cyclam. Tetradentate ligands are ideally suited to accommodate octahedrally coordinated Ni(II) for coordination of two cyano groups in the cyanometallate structures.

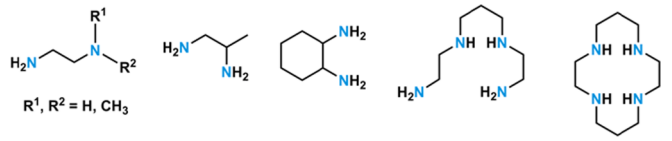

Fig. 1. Amines used as blocking ligands for Ni(II) in cyanometallates. From left to right: ethylenediamine, propane-1,2-diamine, cyclohexane-1,2-diamine, bis (2-aminoethyl)-1,3-propanediamine (2,3,2-tetramine), 1,4,8,11-tetraazacyclotetradecane (cyclam).

2. Results and discussion

2.1. Synthesis of $Si(OR)_3$-substituted blocking ligands

Contrary to AEAPTS, which is commercially available, $Si(OR)_3$-substituted derivatives of the tetramines were hitherto unknown. Modification of *N,N′*-bis(2-aminoethyl) − 1,3-propanediamine (2,3,2-tetramine) by one (trimethoxysilyl)propyl group (resulting in "silyl − 2,3,2-tetramine") was achieved by deprotonation of 2,3,2-tetramine, followed by slow addition of 3-iodopropyltrimethoxysilane (Eq. (1)).

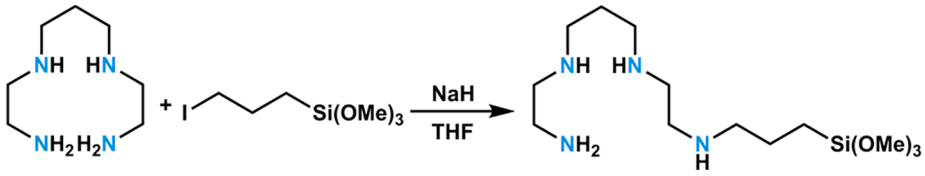

(1)

Modification of 2,3,2-tetramine with two (trimethoxysilyl)propyl groups ("bissilyl − 2,3,2-tetramine") was achieved according to Eq. (2) by reaction of AEAPTS and 1,3-dibromopropane under basic conditions, similar to the synthesis of 2,3,2-tetramine [10], but under water-free conditions to avoid premature hydrolysis of the trimethoxysilyl groups.

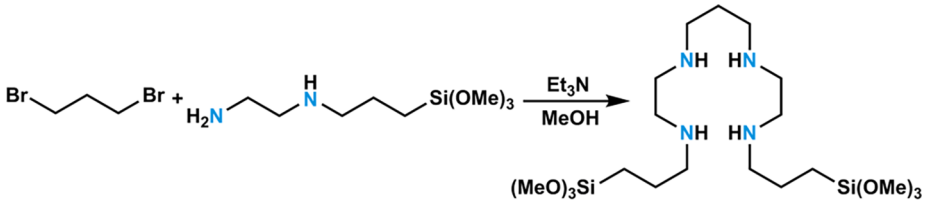

(2)

Cyclam was modified with a (trimethoxysilyl)propyl side chain by reaction with 3-iodopropyltrimethoxysilane after deprotonation with NaH (Eq. (3)). The mono-substituted product ("silylcyclam") was obtained as a mixture with multiply substituted species. The side products, however, constituted only a minor proportion, as proven by ^1H NMR, and further purification deemed unnecessary for the purpose of this work.

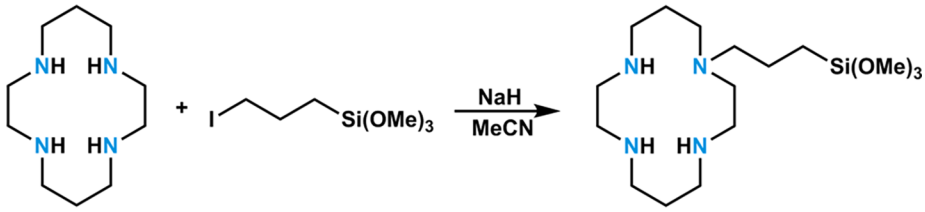

(3)

In order to lower the potential influence of the (trialkoxysilyl)propyl group on the coordination properties of the cyclam moiety, the primary amino group of 6-aminocyclam was also used for modification. This was achieved by addition of 3-isocyanopropyltriethoxysilane to 6-aminocyclam (Eq. (4)). A mixture of mostly the mono-substituted compound ("silyl-6-aminocyclam") with a small proportion of multiply silylated compounds was obtained and used without further purification.

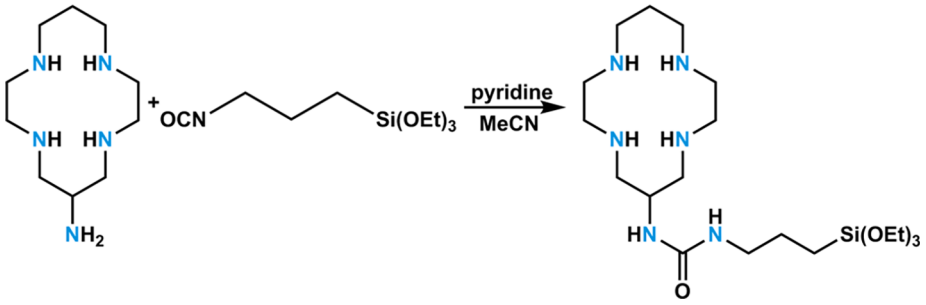

(4)

2.2. $Si(OR)_3$-substituted cyanometallates and sol-gel processing

An example of the reaction sequence for embedding the $Si(OR)_3$-substituted cyanometallate in sol-gel silica is shown in Fig. 2.

The (trialkoxysilyl)propyl-substituted derivatives were first reacted with $NiCl_2$, resulting in the corresponding $[Ni(tetramine)]Cl_2$ complexes. Successful complexation was monitored by the color change of the solution and UV/vis-spectra. Absorptions in the regions 325–400 and 550–700 nm, which are typical for octahedral Ni(II) complexes [11–13], were observed in each case: $[Ni(silyl\text{-}2,3,2\text{-}tetramine)]Cl_2$ showed absorption maxima at 358 and 591 nm, $[Ni(bissilyl\text{-}2,3,2\text{-}tetramine)]Cl_2$ at 361 and 575 nm, $[Ni(silylcyclam)]Cl_2$ at 336, 449 and 652 nm, and $[Ni(silyl\text{-}6\text{-}aminocyclam)]Cl_2$ at 339, 429, 462 and 649 nm.

The reference compounds $[Ni(ethylenediamine)_2]_3[Fe(CN)_6]_2{\cdot}x\,H_2O$ are metamagnets exhibiting field-induced antiferro–ferro–paramagnetic transitions, with huge influence of the number of water molecules (x) [14]. Trialkoxysilyl-substituted cyanometallate derivatives thereof were prepared by reaction of 3 Eq. of the Ni(II) complex with 2 Eq. of $K_3[Fe(CN)_6]$ and embedded in silica by co-reaction with tetraethoxysilane (TEOS) under basic conditions. The cyanometallate-SiO_2 materials obtained by sol-gel processing are named "$[Ni(tetramine)]_x[Fe(CN)_6]_y$ gels".

EDX measurements confirmed a Ni:Fe ratio of about 2.6:2 for $[Ni(silyl\text{-}2,3,2\text{-}tetramine)]_3[Fe(CN)_6]_2$ gel, 2.8:2 for $[Ni(bissilyl\text{-}2,3,2\text{-}tetramine)]_3[Fe(CN)_6]_2$ gel and 2.9:2 for $[Ni(silyl\text{-}6\text{-}aminocyclam)]_3[Fe(CN)_6]_2$ gel. This corresponds quite well to the ideal ratio of 3:2. The excess of Fe may indicate that a part of the $[Fe(CN)_6]^{3-}$ units form less than three cyano bridges to Ni(II) which causes deviation from the ideal stoichiometry. Charge balance is kept by incorporation small proportions of K^+ ions into the material. In contrast, a Ni:Fe ratio of about 1.1:1 was found in the reaction of $[Ni(silylcyclam)]^{2+}$, although a 3:2 ratio of the starting compounds was also employed in this case. This is close to the theoretical 1:1 ratio for a $K[Ni(silylcyclam)][Fe(CN)_6]$ gel. The slight excess of Ni in this case may arise from the fact that unreacted $K_3[Fe(CN)_6]$ can be removed from the material by washing with water while the Ni(II) complex is covalently bound to the SiO_2 matrix through its polyamine ligand.

The FTIR spectra of all cyanometallates and the gels prepared thereof were similar to that of previously described $[Ni(AEAPTS)]_3[Fe(CN)_6]_2$ gel [9]: two bands in the characteristic region of C≡N appear in the spectra of $[Ni(polyamine)]_3[Fe(CN)_6]_2$ and $K[Ni(silylcyclam)][Fe(CN)_6]$, and the derived gels (the latter are shown in Fig. 3). One band corresponds to the non-bridging cyano groups (2090–2115 cm^{-1}) and the other to the bridging cyano groups (2040–2060 cm^{-1}). The presence of the ligand bands, especially the characteristic stretching bands of secondary amines at 3300–3350 and 3200–3260 cm^{-1} in the gels, are another indication that the cyanometallate structure is at least partly retained in the gel. The maxima at around 1075, 1190 and 2840 cm^{-1} in the cyanometallates, characteristic of Si-OCH_3, disappeared after sol-gel

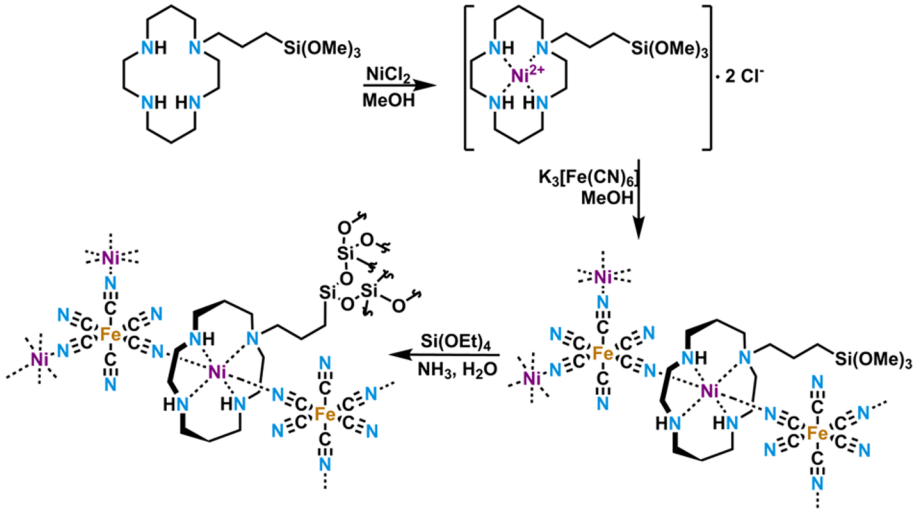

Fig. 2. Synthesis of SiO_2-embedded cyanometallates (with the silylcyclam ligand, as an example).

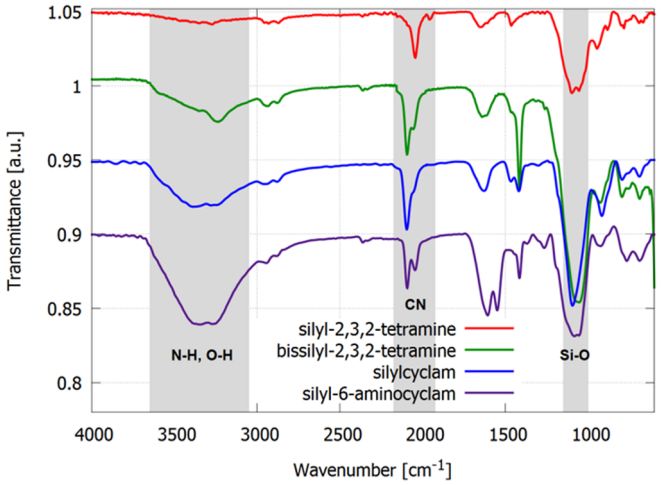

Fig. 3. FTIR spectra of SiO_2-embedded cyanometallates with different tetramine ligands, shifted by 0.05 for clarity.

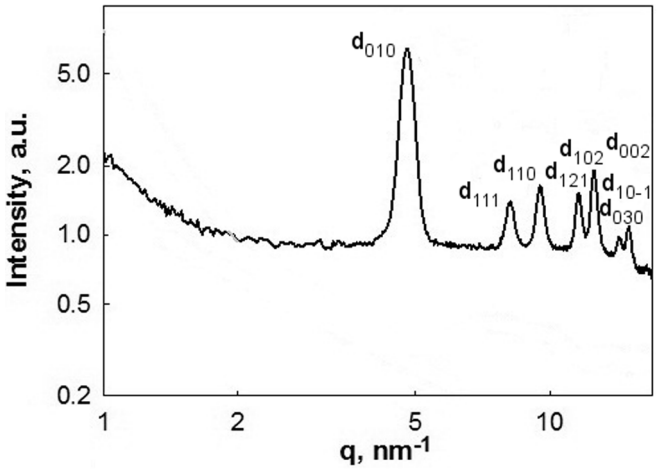

Fig. 4. SWAXS curve of $[Ni(AEAPTS)_2]_3[Fe(CN)_6]_2$ with monoclinic indexing.

processing, indicating successful formation of the silica matrix. The characteristic Si—O—Si band at 1050–1095 cm^{-1} was more intense and broader in the spectrum of the gels.

SEM images at 5000 or 10,000-fold magnification indicated good homogeneity of the $[Ni(tetramine)]_3[Fe(CN)_6]_2$ and $K[Ni(silylcyclam)][Fe(CN)_6]$ gels without discernible phase separation. This excludes the possibility that (micro-)crystallites of the cyanometallates are incorporated in the silica network. This was also confirmed by the SWAXS studies reported in the following paragraph.

2.3. Structural analysis (SWAXS)

Small- and wide-angle X-ray scattering (SWAXS) measurements were performed before and after sol-gel processing to gain insight on how sol-gel processing influences the structural arrangement of the cyanometallate.

2.3.1. Cyanometallate structures before sol-gel processing

All $Si(OR)_3$-modified cyanometallates were microcrystalline and showed distinct Bragg reflections which allowed suggesting a model for the crystal structures of these compounds.

In our Communication on $[Ni(AEAPTS)_2]_3[Fe(CN)_6]_2$ [9] we had reported a satisfactory fit of the Bragg reflections for a hexagonal unit cell which led us to propose a structure with parallel chains arranged along *c*, where two neighboring chains are shifted relative to each other. This was a possible solution for the structure, as the low number of reflections indicated a high symmetry. A lower number of reflections can, however, also be caused by a spatially confined crystallite structure. In the light of the results obtained for the $[Ni(tetramine)]_3[Fe(CN)_6]_2$ derivatives (see below), we re-fitted the Bragg reflections of $[Ni(AEAPTS)_2]_3[Fe(CN)_6]_2$ and also got an excellent agreement for a monoclinic lattice with two (nearly) identical axes, $a \approx c \approx 1040$ pm, $b = 1323$ pm and $\beta = 132.1°$ (Fig. 4 and Table 1). The length of the *a* and *c* axis corresponds to the typical distance of a Fe—C≡N—M(II)—N≡C—Fe unit [15].

Table 1
Fit and experimental peak maxima positions q_{max} for $[Ni(AEAPTS)_2]_3[Fe(CN)_6]_2$. Monoclinic unit cell monoclinic, $a \approx c \approx 1040$ pm, $b = 1323$ pm, $\beta = 132.1°$.

peak	fit	q_{max} [nm^{-1}]
d_{010}	4.749	4.78
d_{111}	8.191	8.16
d_{100}	8.215	
d_{110}	9.489	9.51
d_{020}	9.498	
d_{121}	11.608	11.6
d_{102}	12.513	12.6
d_{120}	12.558	
d_{030}	14.247	14.3
d_{10-1}	15.013	15.0
d_{002}	16.430	16.4
d_{130}	16.446	

Fig. 5 (left) shows the proposed arrangement of $[Ni(AEAPTS)_2]_3[Fe(CN)_6]_2$ with a stacked ladder-like structure. This updated structural model has the advantage that it complies with the 3:2 ratio of Ni(II) and Fe(III). The structure is basically similar to that of $[Ni(ethylenediamine)_2]_3[Fe(CN)_6]_2 \cdot x\ H_2O$ [16] (Fig. 5) with a triclinic unit cell ($a = 970.9(2)$ pm, $b = 1603.6(5)$ pm, $c = 744.5(2)$ pm, $\alpha = 91.81(3)°$, $\beta = 106.72(2)°$, $\gamma = 74.91(2)°$ for x = 2) [8] and composed from double chains with alternating Fe(III) and Ni(II) in one direction. The two strands of such —Fe(III)—C≡N—Ni(II)— chains are connected by —C≡N—Ni(II)—N≡C— bridges. The repeat unit of each double chain are thus three Ni(II) and two Fe(III) alternatingly connected by cyano bridges. This results in a Ni_3Fe_2 stoichiometry with two cyano bridges and two diamine blocking ligands at every Ni(II), and three bridging and three non-bridging cyano groups in *mer* arrangement at every Fe(III). A similar arrangement of double chains with slightly tighter packing and a monoclinic unit cell can be rationalized for $[Ni(AEAPTS)_2]_3[Fe(CN)_6]_2$. The 1D double chains are extending along the *c*-axis, as shown in Fig. 5.

Lattice constants very similar to $[Ni(AEAPTS)_2]_3[Fe(CN)_6]_2$ were obtained for $[Ni(silyl\text{-}2,3,2\text{-}tetramine)]_3[Fe(CN)_6]_2$ and $[Ni(bissilyl\text{-}2,3,2\text{-}tetramine)]_3[Fe(CN)_6]_2$. A fit for a monoclinic unit cell with lattice parameters $a \approx c \approx 1050$ pm, $b = 1310$ pm and $\beta = 133.0°$ is in excellent agreement with the experimental q_{max} values (black curves in Figs. 6 and 7, Table 2). Both compounds have nearly the same unit cells and are isostructural with $[Ni(ethylenediamine)_2]_3[Fe(CN)_6]_2 \cdot x\ H_2O$ and $[Ni(AEAPTS)_2]_3[Fe(CN)_6]_2$.

The SWAXS curve of $K[Ni(silylcyclam)][Fe(CN)_6]$ (black curve in Fig. 8, Table 3) was slightly different, visible by the higher number of Bragg reflections. The minimal change to include also the additional peaks was to choose $\alpha \neq 90°$ but keep $a \approx c$ and $\gamma = 90°$. This is just a small modification of the monoclinic model, but the unit cell becomes triclinic, with $a \approx c \approx 1040$ pm, $b = 1330$ pm, $\alpha = 83.1°$, $\beta = 124.9$, $\gamma = 90.0°$. The deviation of α from 90° is probably the consequence of the bulkier ligands. However, the common structural motif of the three cyanometallates is retained, *i.e.* stacked ladders with the $Si(OR_3)$-substituted groups pointing into the free space at both sides.

$[Ni(silyl-6\text{-}aminocyclam)]_3[Fe(CN)_6]_2$ (black curve in Fig. 9) does

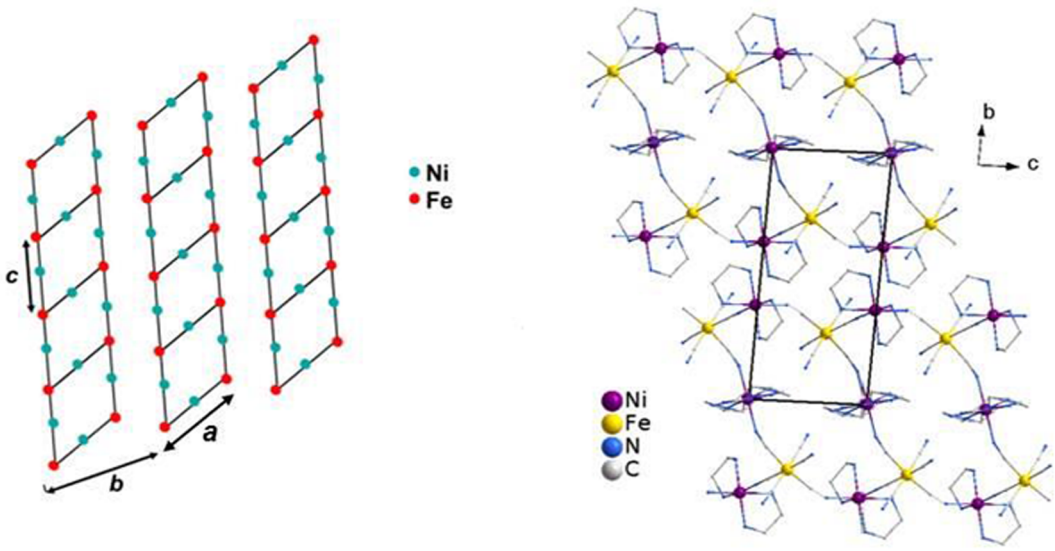

Fig. 5. Left: Proposed structure for $[Ni(AEAPTS)_2]_3[Fe(CN)_6]_2$. The cyanometallates are arranged as stacked ladders. Right: Crystal structure of $[Ni(ethylenediamine)_2]_3[Fe(CN)_6]_2{\cdot}2\ H_2O$ [16].

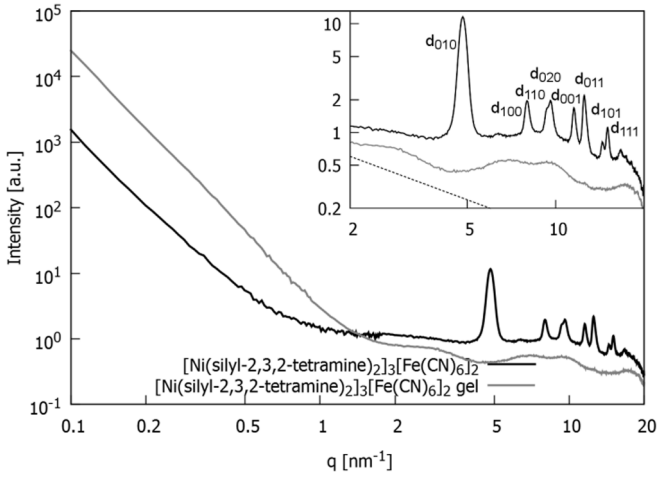

Fig. 6. SWAXS curves of $[Ni(silyl-2,3,2\text{-tetramine})]_3[Fe(CN)_6]_2$ in logarithmic scale. The insert shows an enlargement of the region q = 1–10 nm^{-1}. The dashed line in the insert indicates a slope of q^{-1}. The reflections of are indexed for a monoclinic unit cell.

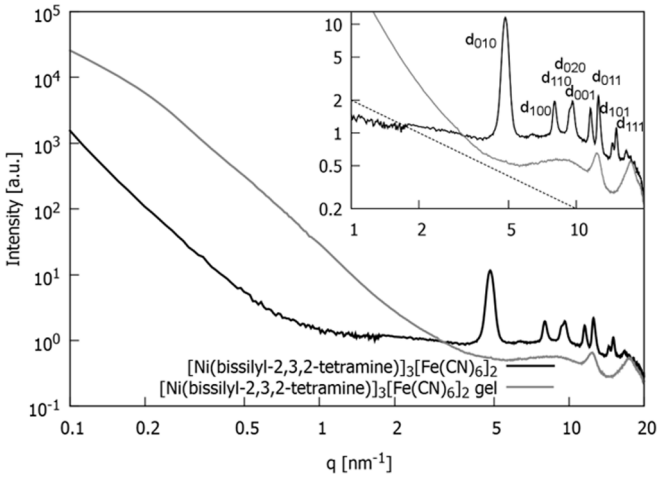

Fig. 7. SWAXS curves of $[Ni(bissilyl\text{-}2,3,2\text{-tetramine})]_3[Fe(CN)_6]_2$ in logarithmic scale. The insert shows an enlargement of the region q = 1–10 nm^{-1}. The dashed line in the insert indicates a slope of q^{-1}. The reflections are indexed for a monoclinic unit cell.

not form a long-range crystalline structure of stacked ladders, visible by the complete absence of the ladder-ladder distance reflection at about q = 4.8 nm^{-1}. However, the broad Bragg reflections at about q = 12.3 nm^{-1} and q = 17.5 nm^{-1} still show that the ladder structure is present. This is also supported by strong Bragg reflections, which are observed at similar q values for $[Ni(ethylenediamine)_2)_2]_3[Fe(CN)_6]_2{\cdot}x\ H_2O$ and induced by the ladder-like structural subunits.

2.3.2. Cyanometallate structures after sol-gel processing

The SWAXS curves of the materials with modified blocking ligands after sol–gel processing (grey curves in Figs. Figs. 6–9) are summarized in Fig. 10. The absence of the peak at about q = 4.8 nm^{-1} again led to the conclusion that no stacking of the ladders is observed. Therefore, the 3D crystalline order of the cyanometallates was destroyed during sol-gel processing.

However, there were still two broad reflections at about q = 12.3 and 17.5 nm^{-1} for some cyanometallates, which characterize the ladder structure. A closer inspection showed that these peaks are absent if the ligand(s) at Ni(II) are asymmetric chains (AEAPTS, silyl-2,3,2-tetramine), but are present for symmetric (bissilyl-2,3,2-tetramine, silylcylam, silyl-6-aminocyclam) ligands. One can therefore conclude that symmetric or silylcyclam ligands lead to a stiffening of the ladder

Table 2
Fit and experimental peak maxima positions q_{max} for $[Ni(silyl\text{-}2,3,2\text{-tetramine})]_3[Fe(CN)_6]_2$ and $[Ni(bissilyl\text{-}2,3,2\text{-tetramine})]_3[Fe(CN)_6]_2$. Monoclinic unit cell, $a \approx c \approx$ 1050 pm, b = 1310 pm, β = 133.0°.

peak	fit	q_{max} [nm^{-1}]
d_{010}	4.798	4.83
d_{100}	8.112	8.00
d_{110}	9.498	9.35
d_{020}	9.595	9.63
d_{121}	11.613	11.6
d_{102}	12.359	12.5
d_{120}	12.620	
d_{030}	14.393	14.5
$d_{10\text{-}1}$	15.033	15.1
d_{002}	16.394	16.5
d_{130}	16.563	

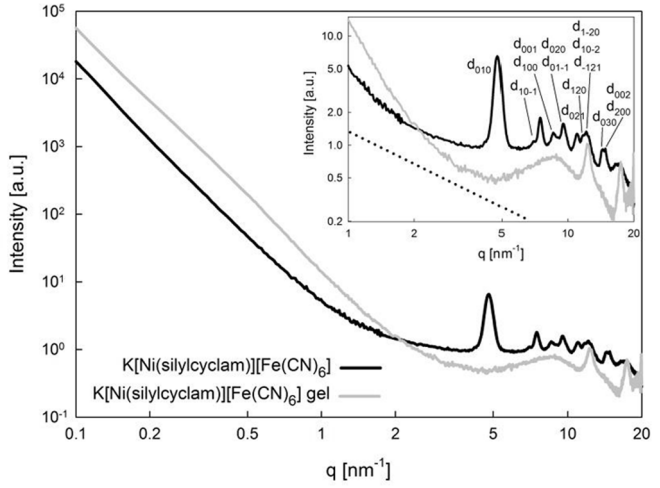

Fig. 8. SWAXS curves of K[Ni(silylcyclam)][Fe(CN)$_6$] in logarithmic scale. The insert shows an enlargement of the region q = 1–10 nm^{-1}. The dashed line in the insert indicates a slope of q^{-1}. The reflections are indexed for a triclinic unit cell.

Table 3
Fit and experimental peak maxima positions q_{max} for K[Ni(silylcyclam)][Fe(CN)$_6$]. Triclinic unit cell, $a \approx c \approx 1040$ pm, b = 1330 pm, α = 83.1°, β = 124.9, γ = 90.0°.

peak	fit	q_{max} [nm^{-1}]
d$_{010}$	4.772	4.80
d$_{10-1}$	6.856	6.82
d$_{100}$	7.378	7.46
d$_{001}$	7.442	
d$_{110}$	8.411	8.56
d$_{11-1}$	8.644	
d$_{01-1}$	9.462	9.52
d$_{020}$	9.544	
d$_{021}$	11.12	11.0
d$_{120}$	11.52	11.6
d$_{12-1}$	12.16	12.4
d$_{10-2}$	12.26	
d$_{1-20}$	12.58	
d$_{030}$	14.32	14.4
d$_{200}$	14.75	14.8
d$_{002}$	14.88	

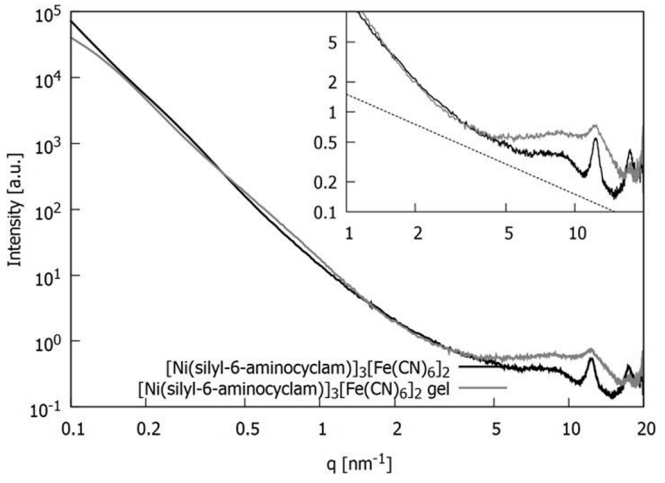

Fig. 9. SWAXS curves of [Ni(silyl-6-aminocyclam)]$_3$[Fe(CN)$_6$]$_2$ in logarithmic scale. The insert shows an enlargement of the region q = 1–10 nm^{-1}. The dashed line in the insert indicates a slope of q^{-1}.

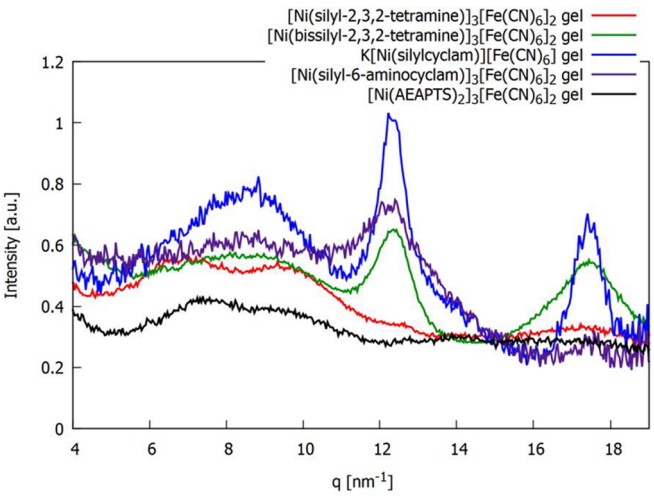

Fig. 10. Summary of SWAXS curves of the gelated cyanometallates.

structure and thus result in Bragg reflections, whereas for asymmetric and small ligands, the reflections disappear. A possible interpretation is that the ligands are asymmetrically distributed around the ladders. This could result in mechanical stress during sol-gel processing (formation of Si—O—Si bonds), with concomitant distortion of the ladder structure and weakening of reflections.

Additionally, there are also some very broad and weak peaks in the q range between 3 and 12 nm^{-1}, which probably arise from the short-range order of silica-rich regions, located in the vicinity of the ladder structure.

Apart from the background from large inhomogeneities at > 100 nm, which produce a q^{-4} increase of the scattering intensity towards very small q values, a q^{-1} intensity decrease in the q range 2–5 nm^{-1} is visible (inserts in Figs. 6–9). This indicates that long, elongated structures are still present, which are preserved during sol-gel processing. These structures could be isolated single or double chains of the cyanometallate.

2.4. Magnetic properties

The magnetic properties of the materials were studied by SQUID measurements at various external fields and temperatures. No magnetic order was found for the materials discussed in this work, in contrast to [Ni(AEAPTS)$_2$]$_3$[Fe(CN)$_6$]$_2$ in silica [9]. This means that all materials are paramagnetic down to at least 2 K (Fig. 11).

The experimental results were corrected for diamagnetic contributions with the theoretical value obtained according to Pascal's method [17]. The effective magnetic moments μ_{eff} were found by fitting a Curie law $\chi_m = C/T$ (where $C = (N\mu_{eff}{}^2\mu_B)/(3k_B)$ is the Curie constant, k_B = Boltzmann constant, N = Avogadro constant, μ_B = Bohr magneton) to the experimental data. This revealed a pronounced influence of the organic ligand and the structural alignment on the magnetic properties (Table 4). All effective moments were below the ones expected for spin-only coupled three Ni(II) and two Fe(III) in a low-spin state (8.94 μ_B) for [Ni(tetramine)]$_3$[Fe(CN)$_6$]$_2$ gels, and for one Ni(II) and one Fe(III) in a low-spin state (4.56 μ_B) for K[Ni(silylcyclam)][Fe(CN)$_6$] gel. The moments slightly increase as the temperature decreases (see the lower part in Fig. 11) which indicates the presence of weak ferromagnetic interactions between Ni(II) and Fe(III). An abrupt decrease of the moment at lower temperatures and the relatively low μ_{eff} values may be attributed to antiferromagnetic interactions between cyanometallate chains present in the material. An underestimation of the diamagnetic contribution from the amorphous silica matrix also cannot be fully ruled out.

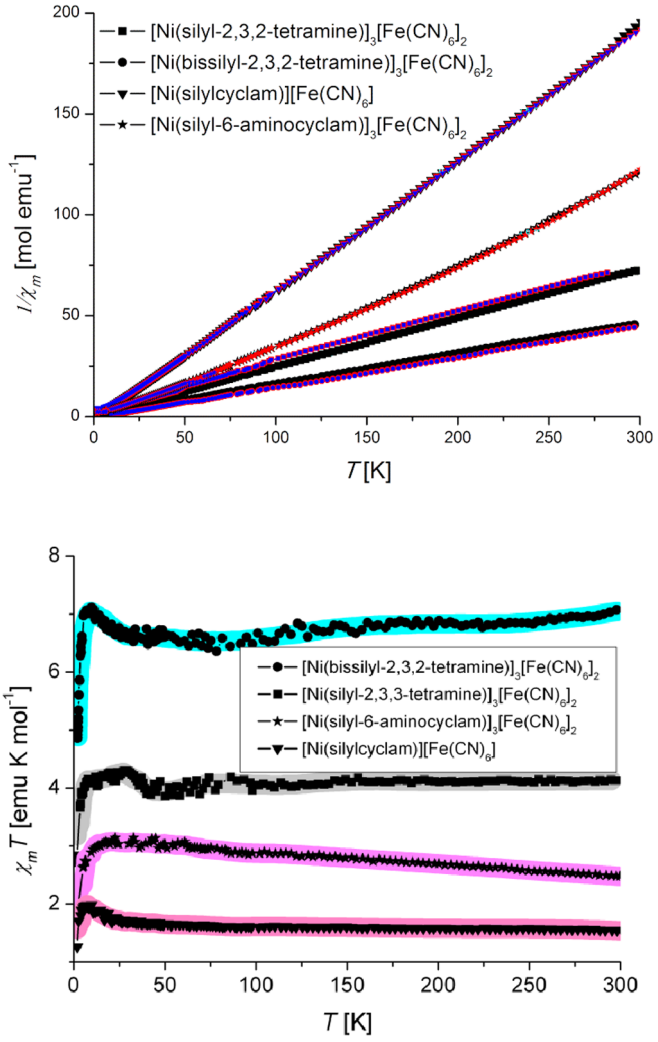

Fig. 11. Top: Inverse magnetic susceptibility (χ_m) *vs.* temperature at various fields: 1 T (black), 3 T (red) and 5 T (blue). Bottom: $\chi_m T$ *vs.* temperature (bottom) for the Ni^{II}–Fe^{III} cyanometallate structures after sol-gel processing. The thick shaded lines are to guide the eye. (For interpretation of the references to color in this figure legend, the reader is referred to the web version of this article.)

Table 4
Magnetism of Ni(II)/Fe(III) cyanometallates in silica.

	magnetism	μ_{eff} [μ_B]	T_c
$[Ni(AEAPTS)]_3[Fe(CN)_6]_2$ gel [9]	ferro	4.46[a]; 8.60[b]	10.6
$[Ni(silyl\text{-}2,3,2\text{-}tetramine)]_3[Fe(CN)_6]_2$ gel	para	5.75 ± 0.09	–
$[Ni(bissilyl\text{-}2,3,2\text{-}tetramine)]_3[Fe(CN)_6]_2$ gel	para	7.12 ± 0.02	–
$K[Ni(silylcyclam)][Fe(CN)_6]$ gel	para	3.56 ± 0.01	–
$[Ni(silyl\text{-}6\text{-}aminocyclam)]_3[Fe(CN)_6]_2$ gel	para	4.64 ± 0.04	–

[a] At room temperature.
[b] Value at maximum below T_c.

3. Conclusions

Ni(II)/Fe(III) cyanometallates with various $Si(OR_3)$-substituted tetramine blocking ligands at Ni(II) were synthesized and embedded in silica by sol–gel processing with $Si(OEt)_4$. Although a $[Ni(tetramine)]^{2+}$:$[Fe(CN)_6]_2^{3-}$ ratio of 3:2 was employed in each case for the cyanometallate synthesis, only $[Ni(silyl-2,3,2\text{-}tetramine)]_3[Fe(CN)_6]_2$, $[Ni(bissilyl\text{-}2,3,2\text{-}tetramine)]_3[Fe(CN)_6]_2$ and $[Ni(silyl\text{-}6\text{-}aminocyclam)]_3[Fe(CN)_6]_2$ had the anticipated stoichiometry, while $K[Ni(silylcyclam)][Fe(CN)_6]$ was obtained under the same conditions. The FTIR spectra of the cyanometallates before and after sol-gel processing clearly showed bands characteristic of both non-bridging and bridging cyano groups and thus proved the formation of Ni(II)−C≡N−Fe(III) bridged cyanometallate networks in each case.

The cyanometallates typically showed distinct Bragg reflections before sol-gel processing indicating high crystallinity. The reflections are consistent with a structure of stacked ladders forming 2D sheets with a monoclinic crystal lattice. This arrangement of double chains is similar to $[Ni(ethylenediamine)_2]_3[Fe(CN)_6]_2 \cdot x\ H_2O$ [16]. Re-fitting of the data of the previously reported compound $[Ni(AEAPTS)_2]_3[Fe(CN)_6]_2$ [9] showed that this compound is isostructural to the newly reported cyanometallates with modified tetramine ligands. The structure of $K[Ni(silylcyclam)][Fe(CN)_6]$ was similar, but a triclinic lattice had to be chosen to take the splitting of some reflections into account. The Bragg reflections characterizing the stacking of the ladders disappeared after sol-gel processing, although some broad Bragg reflections characteristic for the single ladders were identified for bissilyl-2,3,2-tetramine, silylcylam and silyl-6-aminocyclam.

The tetramine-substituted Ni(II)/Fe(III) cyanometallates embedded in SiO_2 were paramagnetic at least down to 2 K, contrary to $[Ni(AEAPTS)]_3[Fe(CN)_6]_2$ gel [9] which showed magnetic order below 22 K, a narrow hysteresis at low temperatures and a positive T_C, indicating ferromagnetic order. The difference in magnetic behavior is probably due to the higher flexibility of the AEAPTS diamine ligands (including *cis/trans* coordination at Ni(II) and/or a higher flexibility of the ladders). This allows the diamine-substituted structure to better adjust to the silica matrix and preserve the ferromagnetic coupling between Ni(II) and Fe(III) ions. Another possible contribution may arise from the structural alignment in the silica-embedded materials. Residual long and elongated structures are still present, as discussed in the SWAXS section. This indicates the preservation of some parts of the ladder structure during sol-gel processing, such as isolated single or double chains of the cyanometallate. Antiferromagnetic coupling between the chains, which is common in such cyanometallate structures [1], may counteract the ferromagnetic exchange between Ni(II) and Fe(III) along the chains.

In conclusion, while the $Si(OR)_3$-substituted blocking ligands did not prevent the formation of mixed-metal cyanometallate structures, sol-gel processing resulted in a loss of crystallinity, *i.e.* the 3D periodic order. This is as expected because otherwise not all $Si(OR)_3$ side groups would have become part of the gel network. The SAXS and FTIR data nevertheless indicate that isolated cyanometallate (double) chains, or segments thereof, were incorporated in the gel network. The results reported in this and previous [9] work show that silica gels with special magnetic properties can be prepared by incorporation of cyanometallate structures in silica although the structural and magnetic properties before and after sol-gel processing do not necessarily correspond. For an optimization of the magnetic properties, deliberate modification of the cyanometallate structure (kind and ratio of the metals) as well as the blocking ligand(s) is necessary.

4. Experimental section

4.1. General methods and materials

Most reagents were obtained from commercial sources and used without further purification. $NiCl_2 \cdot 6H_2O$ was dried at 120 °C to obtain yellow anhydrous $NiCl_2$. *N,N′*-bis(2-aminoethyl)-1,3-propanediamine (2,3,2-tetramine) was synthesized according to Ref. [10], cyclam according to Ref. [18] and 6-aminocyclam according to Ref. [19]. Moisture-free solvents were obtained by subjecting commercial solvents to standard drying techniques and storing over molecular sieves.

4.2. Characterization techniques

^{1}H and ^{13}C NMR spectra in solution were recorded on a Bruker Avance 250 spectrometer (150.13 MHz [^{1}H], 62.86 MHz [^{13}C]) equipped with a 5 mm inverse-broadband probe head and a *z*-gradient unit. FTIR spectra were measured in the range 4000–600 cm^{-1} on a Bruker IR Tensor 27 in ATR mode. UV/Vis spectra were recorded in the range 300–700 nm on a Perkin Elmer Lambda 35 spectrophotometer in aqueous or methanolic solution. SEM were recorded on a FEI Quanta 200 scanning electron microscope with a tungsten filament electron gun at acceleration voltages of 5 or 10 kV. Powder samples were immobilized on carbon tape and sputter-coated with gold. EDX analysis was carried out with an EDAX Genesis energy dispersive spectrometer mounted on the SEM chamber.

Magnetic properties were measured on a S700X SQUID magnetometer (Cryogenic Ltd) on free-powder samples in a gelatin capsule. The magnetic moments were corrected for the diamagnetic background of the capsule. Zero field cooled (ZFC) and field cooled (FC) data were collected in the temperature range 2–300 K with various applied fields. The obtained results were corrected for diamagnetic contributions of the sample by subtraction of theoretical values obtained according to Pascal's method [17].

Small- and wide angle experiments were performed with a Bruker Nanostar, equipped with a 2D-position sensitive detector (Vantec 2000). The scattering patterns were taken typically for 600 s. The radially integrated data were corrected for background scattering, small- and wide-angle data were merged to result in scattering intensities in dependence on the scattering vector $q = (4\pi/\lambda)\sin\theta$ in the range q = 0.1–20 nm^{-1} (2θ = scattering angle, λ = 0.1542 nm).

4.3. Ligand syntheses

4.3.1. N-(3-(trimethoxysilyl)propyl)-2,3,2-tetramine (silyl − 2,3,2-tetramine)

2,3,2-tetramine (3.64 g, 22.73 mmol) was dissolved in 600 mL of THF and cooled in an ice bath under argon atmosphere. NaH (600 mg, 25.00 mmol) was added in small batches and the suspension stirred for 1 h at room temperature. 3-Iodopropyltrimethoxysilane (6.60 g, 22.73 mmol) was added and the reaction heated to reflux overnight. THF was removed under vacuum, the residue dissolved in 10 mL of CH_2Cl_2 and filtrated under argon atmosphere. CH_2Cl_2 was removed under vacuum and the procedure repeated with 5 mL of toluene. Evaporation yielded **1** as a slightly yellow viscous liquid (2.29 g, 31%). ^{1}H NMR (MeOD): δ = 0.54–0.67 (m, 2 H, C*H*$_2$Si), 1.45–1.75 (m, 4 H, C*H*$_2$(CH$_2$NH)$_2$, C*H*$_2$CH$_2$Si), 2.37–2.74 (m, 14 H, C*H*$_2$NH$_2$, C*H*$_2$NH), 3.52 (s, OC*H*$_3$) ppm; ^{13}C NMR ($CDCl_3$): δ = 6.70 (*C*H$_2$Si), 23.21 (*C*H$_2$CH$_2$Si), 29.83 (*C*H$_2$(CH$_2$NH)$_2$), 40.93 (*C*H$_2$NH$_2$), 49.08, 49.67, 50.20, 50.55 (*C*H$_2$NH), 50.12 (O*C*H$_3$), 51.84 (*C*H$_2$CH$_2$CH$_2$Si) ppm; IR: 776 (s), 813 (s), 1074 (s), 1189 (m), 1458 (m), 1593 (w), 2835 (m), 2934 (m), 3254 (w) cm^{-1}.

4.3.2. N,N'-bis(3-(trimethoxysilyl)propyl) − 2,3,2-tetramine (bissilyl − 2,3,2-tetramine)

1,3-dibromopropane (2.14 g, 10.60 mmol) in 10 mL of methanol was added dropwise to [3-(2-aminoethyl-amino)propyl]trimethoxysilane under argon atmosphere. The mixture was then heated to reflux for 1 h. Triethylamine (3.86 g, 38.16 mmol) was added and the solution kept at reflux overnight. A white precipitate was formed upon cooling, which was filtered off under argon atmosphere after solvent removal under vacuum. A yellowish viscous liquid was obtained (1.24 g, 24%). ^{1}H NMR ($CDCl_3$): δ = 0.53–0.72 (m, 4 H, C*H*$_2$Si), 1.50–1.71 (m, 4 H, C*H*$_2$CH$_2$Si), 1.71–1.95 (m, 2 H, C*H*$_2$(CH$_2$NH)$_2$), 2.42–3.13 (m, 16 H, C*H*$_2$NH), 3.52 (s, OC*H*$_3$) ppm; ^{13}C NMR ($CDCl_3$): δ = 6.69 (*C*H$_2$Si), 20.26 (*C*H$_2$(CH$_2$NH)$_2$), 22.67 (*C*H$_2$CH$_2$Si), 40.98 (CH$_2$(*C*H$_2$NH)$_2$), 50.45, 51.39 (*C*H$_2$NH), 50.62 (O*C*H$_3$), 52.04 (*C*H$_2$CH$_2$CH$_2$Si) ppm; IR: 778 (s), 811 (s), 1075 (s), 1189 (m), 1308 (w), 1354 (w), 1411 (w), 1460 (m), 1595 (w), 2838 (m), 2939 (m), 3264 (w) cm^{-1}.

4.3.3. 1-(3-(trimethoxysilyl)propyl) − 1,4,8,11-tetraazacyclotetradecane (silylcyclam)

Cyclam (2.50 g, 12.5 mmol) was suspended in 200 mL of acetonitrile under argon atmosphere. NaH (300 mg, 12.5 mmol) was added in small portions and resulted in the evolution of hydrogen. The resulting mixture was heated to reflux for 1 h. A solution of 3-iodopropyltrimethoxysilane in 100 mL of acetonitrile was subsequently added dropwise and the reaction mixture heated to reflux overnight. The solvent was removed under reduced pressure and the residue washed three times with CH_2Cl_2 (~60 mL) and filtered. To obtain the modified cyclam as a brownish oil (4.13 g, 11.45 mmol, 92%) CH_2Cl_2 was removed under reduced pressure. ^{1}H NMR ($CDCl_3$): δ = 0.44–0.70 (m, 2 H, C*H*$_2$Si), 1.36–1.88 (m, 6 H, C*H*$_2$CH$_2$Si, C*H*$_2$(CH$_2$N)$_2$), 2.26–3.17 (m, 18 H, C*H*$_2$N), 3.47–3.58 (s, 9 H, C*H*$_3$OSi) ppm, broad peaks indicating mixture of multiply substituted derivatives; ^{13}C NMR ($CDCl_3$): δ = 8.6 (*C*H$_2$Si), 18.9 (*C*H$_2$CH$_2$Si), 26.9, 29.6 (*C*H$_2$(CH$_2$NH)$_2$), 48.4, 48.7, 49.6, 50.0, 50.1, 51.6, 53.9, 55.2, 56.1 (*C*H$_2$N, *C*H$_3$OSi), 58.9 (NCH$_2$CH$_2$CH$_2$Si) ppm; IR: 695 (w), 814 (s), 1072 (s), 1189 (m), 1300 (w), 1364 (w), 1461 (m), 1600 (m), 1638 (w), 2186 (w), 2810 (w), 2837 (w), 2939 (s), 3201 (w), 3305 (w) cm^{-1}.

4.3.4. 1-(1,4,8,11-tetraazacyclotetradecane) − 3-(3-(triethoxysilyl)propyl) urea (silyl − 6-aminocyclam)

6-Aminocyclam (0.5 g, 2.32 mmol) was suspended in 200 mL of acetonitrile and 60 mL of pyridine. 3-Isocyanopropyltrimethoxysilane (0.57 g, 0.57 mL, 2.32 mmol) in 10 mL of MeCN was added dropwise. The reaction mixture was heated to reflux overnight and then filtered. Silyl-6-aminocyclam was obtained after solvent removal and drying as light brown very viscous liquid (1.04 g, 2.25 mmol, 97%). ^{1}H NMR ($CDCl_3$): δ = 0.54–0.69 (t, 2 H, C*H*$_2$-Si), 1.14–1.25 (t, 9 H, SiOCH$_2$C*H*$_3$), 1.48–1.69 (m, 2 H, SiCH$_2$C*H*$_2$), 1.69–2.03 (m, 2 H, C*H*$_2$(CH$_2$NH)$_2$), 2.34–3.58 (m, 19 H, C*H*$_2$NH, C*H*NH), 3.71–3.90 (q, 6 H, SiOC*H*$_2$CH$_3$) ppm; ^{13}C NMR ($CDCl_3$): δ = 13.47 (SiCH$_2$CH$_2$), 18.46 (SiOCH$_2$*C*H$_3$), 22.28 (*C*H$_2$(CH$_2$NH)$_2$), 24.85 (SiCH$_2$CH$_2$), 42.38 (NHCH$_2$*C*H$_2$NH), 44.64 (CH$_2$(*C*H$_2$NH)$_2$), 45.68 (SiCH$_2$CH$_2$*C*H$_2$), 52.22 (NHC(O)CH*C*H$_2$), 57.91 (NHC(O)*C*H), 58.48 (SiO*C*H$_2$CH$_3$), 157.62 (*C*=O) ppm; IR: 681 (w), 765 (m), 953 (m), 1073 (s), 1101 (s), 1165 (m), 1190 (w), 1264 (s), 1293 (s), 1365 (w), 1389 (w), 1407 (w), 1441 (w), 1536 (m), 1624 (m), 2885 (m), 2926 (m), 2972 (m), 3294 (w) cm^{-1}.

4.4. Synthesis of [Ni(tetramine)]Cl_2 complexes

One equivalent of the tetramine ligand in 8 mL/mmol of ethanol was slowly added to a heated solution (50 °C) of $NiCl_2$ (1 Eq.) in 15 mL/mmol of ethanol. The reaction solution was stirred 1 h at 50 °C and then concentrated. The resulting precipitate was filtering off, washed with diethyl ether and dried under vacuum. Yield ~70%.

[Ni(silyl-2,3,2-tetramine)]Cl_2: bright violet powder; IR: 691 (w), 800 (s), 880 (m), 1054 (s), 1190 (m), 1262 (w), 1463 (m), 2931 (m), 3152 (m) cm^{-1}.

[Ni(bissilyl-2,3,2-tetramine)]Cl_2: brown powder; IR: 646 (w), 679 (w), 785 (s), 813 (s), 896 (w), 971 (m), 1072 (s), 1190 (s), 1277 (w), 1316 (w), 1460 (m), 1591 (w), 2840 (m), 2942 (m), 3244 (m) cm^{-1}.

[Ni(silylcyclam)]Cl_2: brown powder; IR: 688 (w), 811 (s), 1069 (s), 1190 (m), 1261 (w), 1457 (m), 1591 (m), 2840 (m), 2944 (m) cm^{-1}.

[Ni(silyl-6-aminocyclam)]Cl_2: brown powder; IR: 680 (w), 781 (m), 949 (m), 1072 (s), 1166 (m), 1262 (s), 1509 (s), 1613 (s), 2880 (m), 2926 (m), 2970 (m), 3217 (m), 3315 (w) cm^{-1}.

4.5. Cyanometallate synthesis

A heated solution of $K_3[Fe(CN)_6]$ (2 Eq.) in 65 mL/mmol of methanol was slowly added to a heated (50 °C) solution of [Ni(tetramine)]Cl_2 (3 Eq.) in 40 mL/mmol of methanol. A precipitate formed immediately and was filtered off, washed with ethanol and dried under vacuum. The cyanometallate was obtained quantitatively.

[Ni(silyl-2,3,2-tetramine)]$_3$[Fe(CN)$_6$]$_2$: brown powder; IR: 879 (w), 956 (m), 1062 (s), 1192 (w), 1262 (m), 1435 (w), 1590 (w), 1664 (w), 1786 (w), 2043 (m), 2117 (m), 2878 (m), 2925 (m), 3146 (m) cm^{-1}.

[Ni(bissilyl − 2,3,2-tetramine)]$_3$[Fe(CN)$_6$]$_2$: brown powder; IR: 688 (w), 802 (m), 971 (m), 1072 (s), 1415 (m), 1610 (w), 2057 (s), 2094 (s), 2840 (m), 2942 (m), 3244 (m) cm^{-1}.

K[Ni(silylcyclam)][Fe(CN)$_6$]: brown powder; IR: 687 (w), 753 (w), 797 (w), 913 (m), 1093 (s), 1196 (s), 1418 (m), 1465 (m), 1622 (m), 2095 (s), 2876 (w), 2942 (w), 3240 (m), 3367 (m) cm^{-1}.

[Ni(silyl-6-aminocyclam)]$_3$[Fe(CN)$_6$]$_2$: brown powder; IR: 679 (w), 771 (m), 953 (m), 1074 (s), 1164 (w), 1193 (w), 1261 (w), 1387 (w), 1447 (w), 1543 (m), 1622 (m), 2059 (m), 2091 (s), 2880 (m), 2929 (m), 2972 (m), 3266 (m), 3340 (m) cm^{-1}.

4.6. Sol-gel processing

[Ni(tetramine)]$_3$[*Fe*(*CN*)$_6$]$_2$ (1 Eq.) and Si(OEt)$_4$ (2 Eq.) were dispersed in 330 mL/(mg network) of 0.2 M NH_3 and stirred for 2 days at 70 °C. The reaction mixture was cooled to room temperature, allowed to dry on a glass plate and then scraped off. Fine powders were obtained in quantitative yield.

[Ni(silyl-2,3,2-tetramine)]$_3$[Fe(CN)$_6$]$_2$ gel: brown powder; IR: 690 (w), 797 (m), 929 (m), 1071 (s), 1415 (s), 1641 (m), 2057 (s), 2094 (s), 2879 (w), 2934 (m), 3235 (m) cm^{-1}; EDX: C 60.74%, N 13.66%, O 12.18%, Si 8.32%, Fe 2.01%, Ni 2.58%; paramagnetic; C = 3.64 emu K mol^{-1}; μ_{eff} = 5.75 ± 0.09 μ_B.

[Ni(bissilyl-2,3,2-tetramine)]$_3$[Fe(CN)$_6$]$_2$ gel: brown powder; IR: 668 (w), 692 (w), 784 (m), 883 (m), 946 (s), 1056 (s), 1098 (s), 1464 (m), 1647 (m), 1958 (w), 2045 (s), 2088 (w), 2871 (m), 2931 (m), 2956 (m), 3270 (m) cm^{-1}; EDX: C 56.86%, N 12.29%, O 10.79%, Si 9.5%, Fe 3.81%, Ni 5.42%; paramagnetic; C = 5.80 emu K mol^{-1}; μ_{eff} = 7.12 ± 0.02 μ_B.

K[Ni(silylcyclam)][Fe(CN)$_6$] gel: brown powder; IR: 869 (w), 795 (w), 916 (m), 1095 (s), 1301 (w), 1418 (m), 1466 (m), 1626 (m), 2096 (s), 2879 (w), 2950 (w), 3277 (m), 3378 (m) cm^{-1}; EDX: C 38.41%, N 34.67%, O 18.37%, Si 3.60%, Cl 0.25%, K 1.12%, I 0.20%, Fe 1.62%, Ni 1.76%; paramagnetic; C = 1.39 emu K mol^{-1}; μ_{eff} = 3.56 ± 0.01 μ_B.

[Ni(silyl-6-aminocyclam)]$_3$[Fe(CN)$_6$]$_2$ gel: brown powder; IR: 689 (w), 767 (w), 945 (w), 1056 (s), 1083 (s), 1265 (w), 1371 (w), 1415 (m), 1549 (s), 1607 (s), 2046 (m), 2093 (m), 2884 (w), 2945 (w), 3270 (s), 3347 (s) cm^{-1}; EDX: C 38.77%, N 31.99%, O 19.77%, Si 5.31%, K 0.61%, Fe 1.47%, Ni 2.08%; paramagnetic; C = 2.24 emu K mol^{-1}; μ_{eff} = 4.64 ± 0.04 μ_B.

Acknowledgements

E.F., U.S., J.A. and H.P. thank the *Fonds zur Förderung der wissenschaftlichen Forschung* (FWF) (projects W1243 and I449) for financial support. A.S. and S.P. acknowledge funding from the European Research Council (FP7-ERC-227378).

References

[1] Review article, E.V. Alexandrov, A.V. Virovets, V.A. Blatov, E.V. Peresypkina, Chem. Rev. 115 (2015) 12286–12319.
[2] Review article, M. Atanasov, P. Comba, S. Hausberg, B. Martin, Coord. Chem. Rev. 253 (2009) 2306–2314.
[3] Review article, J.M. Herrera, A. Bachschmidt, F. Villain, A. Bleuzen, V. Marvaud, W. Wernsdorfer, M. Verdaguer, Philos. Trans. R. Soc. A 366 (2008) 127–138.
[4] Review article, J.M. Herrera, A. Bachschmidt, F. Villain, A. Bleuzen, V. Marvaud, W. Wernsdorfer, M. Verdaguer, Philos. Trans. R. Soc. A 366 (2008) 127–138.
[5] Review article, J.-N. Rebilly, T. Mallah, Struct. Bond. 122 (2006) 103–131.
[6] R. Moulin, E. Delahaye, A. Bordage, E. Fonda, J.-P. Baltaze, P. Beaunier, E. Riviere, G. Fornasieri, A. Bleuzen, Eur. J. Inorg. Chem. (2017) 1303–1313.
[7] L. Lartigue, S. Oh, E. Prouzet, Y. Guari, J. Larionova, Mater. Chem. Phys. 132 (2012) 438–445.
[8] R. Turgis, G. Arrachart, C. Delchet, C. Rey, Y. Barré, S. Pellet-Rostaing, Y. Guari, J. Larionova, A. Grandjean, Chem. Mater. 25 (2013) 4447–4453.
[9] E. Felbermair, A. Sidorenko, S. Paschen, J. Akbarzadeh, H. Peterlik, U. Schubert, Chem. Eur. J. 20 (2014) 9212–9215.
[10] J. Van Alphen, Recl. Trav. Chim. Pays-Bas 55 (1936) 412–418.
[11] J.D. Vitiello, E.J. Billo, Inorg. Chem. 19 (1980) 3477–3481.
[12] F. Négrier, E. Marceau, M. Che, J.M. Giraudon, L. Gengembre, A. Löfberg, J. Phys. Chem. B 109 (2005) 2836–2845.
[13] K.-Q. Sun, E. Marceau, M. Che, Phys. Chem. Chem. Phys. 8 (2006) 1731–1738.
[14] R. Herchel, J. Tuček, Z. Trávníček, D. Petridis, R. Zbořil, Inorg. Chem. 50 (2011) 9153–9163.
[15] J.F. Keggin, F.D. Miles, Nature 137 (1936) 577–578.
[16] M. Ohba, N. Maruono, H. Okawa, T. Enoki, J.M. Latour, J. Am. Chem. Soc. 116 (1994) 11566–11567.
[17] K.-H. Hellwege, A.M. Hellwege (Eds.), Landolt-Börnstein, Vol. 12a Springer, Berlin, 1984pp. 4–5, 12–14.
[18] A. Prokhorov, N. Le Bris, H. Bernard, G. Claudon, H. Handel, Synth. Commun. 36 (2006) 3271–3282.
[19] E. Kimura, M. Shionoya, Y. Iitakag, A. Hino, Inorg. Chem. 32 (1993) 2779–2784.